

A High-Fat Diet Increases Influenza A Virus-Associated Cardiovascular Damage

Jurre Y. Siegers,¹ Boris Novakovic,² Katina D. Hulme,³ Rebecca J. Marshall,³ Conor J. Bloxham,⁴ Walter G. Thomas,⁴ Melissa E. Reichelt,⁴ Lonneke Leijten,¹ Peter van Run,¹ Karen Knox,⁵ Kamil A. Sokolowski,⁵ Brian W. C. Tse,⁵ Keng Yih Chew,³ Angelika N. Christ,⁶ Greg Howe,⁶ Timothy J. C. Bruxner,⁶ Mario Karolyi,⁷ Erich Pawelka,⁷ Rebecca M. Koch,⁸ Rosa Bellmann-Weiler,⁹ Francesco Burkert,⁹ Günter Weiss,⁹ Romit J. Samanta,¹⁰ Peter J. M. Openshaw,¹¹ Helle Bielefeldt-Ohmann,^{3,12} Debby van Riel,^{1,a,①} and Kirsty R. Short^{3,12,a}

¹Department of Viroscience, Erasmus Medical Center, Rotterdam, the Netherlands, ²Epigenetics Research, Murdoch Children's Research Institute and Department of Paediatrics, University of Melbourne, Parkville, Australia, ³School of Chemistry and Molecular Biosciences, The University of Queensland, Brisbane, Australia, ⁴School of Biomedical Science, The University of Queensland, Brisbane, Australia, ⁵Preclinical Imaging Facility, Translational Research Institute Australia, Brisbane, Australia, ⁶Institute for Molecular Bioscience, The University of Queensland, Brisbane, Australia, ⁷Department for Infectious Diseases, Kaiser Franz Josef Hospital, Vienna, Austria, ⁸Radboud University Medical Center, Department of Intensive Care Medicine, Nijmegen, the Netherlands, ⁹Department of Internal Medicine II, Medical University of Innsbruck, Innsbruck, Austria, ¹⁰Department of Medicine, University of Cambridge School of Clinical Medicine, Cambridge, United Kingdom, ¹¹Respiratory Infection Section, National Heart and Lung Institute, Imperial College London, London, United Kingdom, and ¹²Australian Infectious Diseases Research Centre, The University of Queensland, Brisbane, Australia

Background. Influenza A virus (IAV) causes a wide range of extrarespiratory complications. However, the role of host factors in these complications of influenza virus infection remains to be defined.

Methods. Here, we sought to use transcriptional profiling, virology, histology, and echocardiograms to investigate the role of a high-fat diet in IAV-associated cardiac damage.

Results. Transcriptional profiling showed that, compared to their low-fat counterparts (LF mice), mice fed a high-fat diet (HF mice) had impairments in inflammatory signaling in the lung and heart after IAV infection. This was associated with increased viral titers in the heart, increased left ventricular mass, and thickening of the left ventricular wall in IAV-infected HF mice compared to both IAV-infected LF mice and uninfected HF mice. Retrospective analysis of clinical data revealed that cardiac complications were more common in patients with excess weight, an association which was significant in 2 out of 4 studies.

Conclusions. Together, these data provide the first evidence that a high-fat diet may be a risk factor for the development of IAV-associated cardiovascular damage and emphasizes the need for further clinical research in this area.

Keywords. influenza; cardiac disease; extrarespiratory complications; high-fat diet; obesity; overweight; body mass index.

The 2009 influenza virus (IAV) pandemic infected 24% of the global population, resulting in > 500 000 deaths [1]. During this pandemic, overweight (body mass index [BMI] ≥ 25), obesity (BMI ≥ 30), and morbid obesity (BMI ≥ 35) emerged as novel risk factors for severe influenza [2–8]. Moreover, mice fed a high-fat diet (HF mice) are more susceptible to severe respiratory disease following IAV infection [9]. This susceptibility has been associated with altered interferon and cytokine production, impaired leukocyte function, and a reduced response to antigen stimulation in overweight individuals [9–11].

Whilst primarily a respiratory pathogen, IAV is often associated with extrarespiratory complications, the most frequent of which are cardiovascular and central nervous system disease [12–15]. Cardiac complications include endocarditis, myocarditis, and myocardial infarction [12]. For example, in the first 7 days after laboratory-confirmed IAV infection, hospitalization for acute myocardial infarction is 6 times higher than a control interval [16]. However, the role of host factors in IAV-associated heart disease remains to be elucidated.

At present, no study has investigated the role of a high-fat diet in IAV-associated cardiovascular damage. This is in spite of the fact that a high-fat diet and excess weight are associated with both increased influenza severity and increased cardiovascular disease in the absence of a viral infection. Given that > 1.9 billion people are currently overweight/obese [17], the role of excess weight in IAV-associated cardiovascular damage is essential information for patient management as well as pandemic preparedness.

Here, we provide the first evidence that a high-fat diet decreases the antiviral response to IAV whilst increasing IAV replication and structural changes to the heart in mice. These data further advance our understanding of the systemic pathogenesis of influenza.

Received 7 February 2020; editorial decision 27 March 2020; accepted 2 April 2020; published online April 4, 2020.

①D. v. R. and K. R. S. contributed equally to the study.

Presented in part: Australian Virology Society Meeting, Queenstown, New Zealand, 2–5 December 2019; and 8th Orthomyxovirus Research Conference, Hanoi, Vietnam, 12–14 September 2018.

Correspondence: Kirsty R. Short, PhD, School of Chemistry and Molecular Biosciences, The University of Queensland, 68 Cooper Road, St Lucia, Queensland 4066, Australia (k.short@uq.edu.au).

The Journal of Infectious Diseases® 2020;222:820–31

© The Author(s) 2020. Published by Oxford University Press for the Infectious Diseases Society of America. All rights reserved. For permissions, e-mail: journals.permissions@oup.com. DOI: [10.1093/infdis/jiaa159](https://doi.org/10.1093/infdis/jiaa159)

MATERIALS AND METHODS

Cells

Madin Darby Canine Kidney (MDCK) cells were obtained from ATCC and used between passages 20 and 50. Cells were cultured in a humidified incubator at 37°C with 95% O₂ and 5% CO₂.

IAV Strain

Virus stocks of A/H1N1/Auckland/1/2009(H1N1) (Auckland/09) were prepared in embryonated chicken eggs and titers of infectious virus were determined by plaque assays on MDCK cells [18].

Mice

Four-week-old C57BL/6 male and female mice were obtained from the Animal Resources Centre (Australia). Mice were then randomly assigned to be fed either a high-fat diet (HF mice) consisting of 40% calories from fat or a low-fat diet (LF mice) consisting of 12% calories from fat (Specialty Feeds) for 10 weeks and supplied with water ad libitum. All animal work was approved by the University of Queensland Animal Ethics Committee (071/17).

IAV Inoculation of Mice

Mice were anesthetized with isoflurane then inoculated intranasally with 5500 or 100 plaque forming units (PFU) of influenza egg-grown A/Auckland/09(H1N1) or naive allantoic fluid (NAF) in 50 µL.

Blood Oxygen Saturation

Blood oxygen saturation was measured using a MouseOx Plus collar oximeter (Starr).

Body Composition

Whole body composition of live mice was determined using a nuclear magnetic resonance analyzer, Minispec LF50H (Bruker Optik).

Echocardiography

Cardiac function was assessed using a Vevo 2100 high-frequency ultrasound system with a 40 MHz center frequency transducer (Visualsonics). Depilated mice were anesthetized by 1.5% isoflurane, kept warm on a heated stage, with respiration and heart rate monitored on echocardiography (ECG) pads. ECG analysis is described in the [Supplementary Material](#).

Viral Titers

Tissues were collected in DMEM (Gibco) and homogenized using a Qiagen Tissuelyser II (Qiagen). The homogenate was centrifuged and the supernatant collected and stored at -80°C. Viral titers were then measured by plaque assay on MDCK cells [18].

Histology

Hearts were fixed in 10% neutral-buffered formalin, processed to paraffin, and 5-µm sections were stained with H&E. Left ventricular thickness was measured by viewing the sections with a 4× objective with projection to a computer screen and then measuring the left ventricular width in mm. Measurements were performed by a veterinary pathologist (H.B.O.) blinded to treatment groups.

Immunohistochemistry

Immunolabeling for HIF-1α was performed as previously described [19, 20]. Assessment of labelling distribution and intensity are described in the [Supplementary Material](#).

RNA Extraction and cDNA Synthesis

RNA was extracted using NucleoZOL (Macherey-Nagel) and an RNAeasy plus Minielute kit (Qiagen). cDNA for host expression analysis and viral mRNA quantification was synthesized using oligo(dT) (Roche) and a High Capacity cDNA Reverse Transcription Kit (Applied Biosystems). Quantitative polymerase chain reaction (qPCR) was performed using SYBR green (Applied Biosystems). The relevant primers are listed in [Supplementary Table 1](#). Gene expression was normalized relative to glyceraldehyde 3-phosphate dehydrogenase (GAPDH) expression and fold change was calculated using the $\Delta\Delta Ct$ method relative to NAF-infected animals. Outliers were removed using Grubbs outlier test. Viral copy number was determined as previously described [21].

RNA-seq Library Preparation and Sequencing

Library preparation and sequencing was performed at the Institute for Molecular Bioscience Sequencing Facility, University of Queensland. RNA-Seq libraries were generated using the Illumina TruSeq Stranded mRNA LT Sample Prep Kit (Illumina, RS-122-2101/RS-122-2102). Sequencing was performed using the Illumina NextSeq500 (NextSeq control software v2.1.0/Real Time Analysis v2.4.11). The library pool was diluted and denatured according to the standard NextSeq protocol and sequenced to generate single-end 76 bp reads using a 75 cycle NextSeq500/550 High Output reagent Kit v2 (Illumina). Analysis of RNA-seq data is described in the [Supplementary Material](#).

Serum Cytokines

Serum samples were screened for proinflammatory cytokines using the mouse antiviral response LegendPlex according to the manufacturer's instructions (Biolegend). Outliers were removed using Grubbs outlier test.

Patient Data

Data on IAV patients were obtained from previously published sources [22–25]. Patients were excluded from the analysis if

their BMI < 20, as low BMI may be associated with cardiovascular disease [26].

Statistics and Data Availability

Statistical analyses were performed using GraphPad Prism. Full details of statistical analysis and data availability can be found in the [Supplementary Material](#).

RESULTS

A High-Fat Diet in Mice Results in Increased Body and Fat Weight

To study the effect of excess weight on IAV-associated cardiovascular damage, mice were fed either a high-fat or low-fat diet for 10 weeks. Following 10 weeks of a differential diet, HF mice had significantly greater body weight and fat percentage compared to LF mice ([Supplementary Figure 1A and 1B](#)). A small but significant increase in lean weight was also observed in HF mice ([Supplementary Figure 1C](#)). This was accompanied by a decreased heart weight in HF mice, consistent with the fact that muscle weighs more than fat ([Supplementary Figure 1D](#)). Together, these data demonstrate that a high-fat diet for 10 weeks is sufficient to generate a murine model of excess weight.

HF Mice Are More Susceptible to Severe Respiratory Disease Following IAV Infection

We next sought to characterize the pulmonary response to IAV in HF and LF mice. To do so in a comprehensive manner, mice were infected with either a high dose (5500 PFU) or a low dose (100 PFU) of Auckland/09(H1N1) and euthanized at 4 days (high dose) or 6 days (low dose) post infection. Following IAV infection, there was a significant difference in percentage weight loss between HF and LF mice after a low-dose IAV infection (4 days post infection [dpi]; [Figure 1A](#)). Consistent with these data, HF mice had significantly lower blood oxygen saturation at 4 dpi (high dose) and 6 dpi (low dose) compared to LF mice ([Figure 1B](#)). At both viral inoculums and time points there was increased alveolar inflammation in HF mice ([Figure 1C](#)). HF mice infected with 100 PFU of IAV also had a small but significant increase in pulmonary viral load at 6 dpi relative to LF mice ([Figure 1D](#)). Together, these data are consistent with previous findings [27] that HF mice are more susceptible to respiratory disease after IAV infection than LF mice.

To gain a deeper insight into the localized response to IAV, RNAseq was performed on uninfected and infected lung tissue from HF and LF mice 2 dpi with 5500 PFU of IAV ([Supplementary Figure 2](#)). This timepoint and viral inoculum was selected to capture the early transcriptional events in the lungs of infected mice. The effects of a high-fat diet on gene expression in the lungs of mice, in the absence of IAV, have been established [28–30]. Consistent with these findings, several differentially expressed genes were noted when the lung transcriptome of NAF-infected HF and LF mice were compared ([Supplementary Table 2](#)). However, as the focus of the present

study is the specific effects of IAV in different metabolic backgrounds, gene expression data in IAV-infected mice were analyzed relative to the relevant uninfected controls ([Figure 2](#)). In general, LF mice showed a stronger transcriptional response to IAV compared to HF mice ([Figure 2A](#) and [2B](#)). Pathway analyses of differentially expressed genes indicated that the majority of genes were associated with immune system function and that these were poorly expressed in HF mice following IAV infection ([Figure 2B](#)). qPCR confirmed the validity of these analyses at 2 dpi ([Figure 2C](#)). Taken together, these data show that HF mice fail to induce the same number and mRNA levels of proinflammatory mediators in the lung early after IAV infection.

Serum Cytokine Levels Are Reduced in HF Mice After IAV Infection

The immunological response in the respiratory system to IAV in HF mice has been well described early (in this study) as well as later during infection [31]. However, there is currently limited information available on the inflammatory response to IAV outside of the respiratory tract. Therefore, serum cytokines in both LF and HF mice after IAV infection were assessed at 2 dpi (5500 PFU) and 6 dpi (100 PFU) ([Figure 3](#)). At 2 dpi, levels of interleukin-6 (IL-6), interferon- γ (IFN- γ), IFN- α , and IFN- γ inducible protein-10 (IP-10) were significantly higher in IAV-infected LF mice compared to the uninfected LF mice, whilst this was not observed in IAV-infected HF mice when compared to uninfected HF mice ([Figure 3A](#)). Moreover, at 2 dpi, LF mice infected with IAV had significantly higher serum levels of IP-10 compared to IAV-infected HF mice ([Figure 3A](#)). At 6 dpi, monocyte chemoattractant protein-1 (MCP-1), IL-6, IFN- γ , IP-10, and tumor necrosis factor- α (TNF- α) were significantly higher in IAV-infected LF mice compared to uninfected LF mice, whilst this was only observed with MCP-1 in IAV-infected HF mice when compared to uninfected HF mice ([Figure 3B](#)). Overall, these observations are consistent with a decreased proinflammatory response to IAV in the serum of HF mice.

The Antiviral Response in the Heart Is Reduced in HF Mice After IAV Infection

The above data suggest that, in addition to a differential respiratory response to IAV, HF and LF mice also display a differential systemic response to IAV. To further study extrarespiratory responses, we first investigated the replication of IAV outside of the respiratory tract of HF and LF mice at 2 dpi (5500 PFU). IAV was not detected in the brain, spleen, pancreas, tracheobronchial lymph nodes, duodenum, jejunum, ileum, and blood, whilst virus was sporadically detected in the kidney, liver, and adrenal gland at low titers (data not shown). However, in both LF and HF mice, virus was consistently detected in the heart at 2 dpi ([Figure 4A](#)). Similarly, infectious virus was detected in the hearts of LF and HF mice at 6 dpi following infection with 100 PFU of IAV ([Figure 4A](#)). Strikingly, significantly

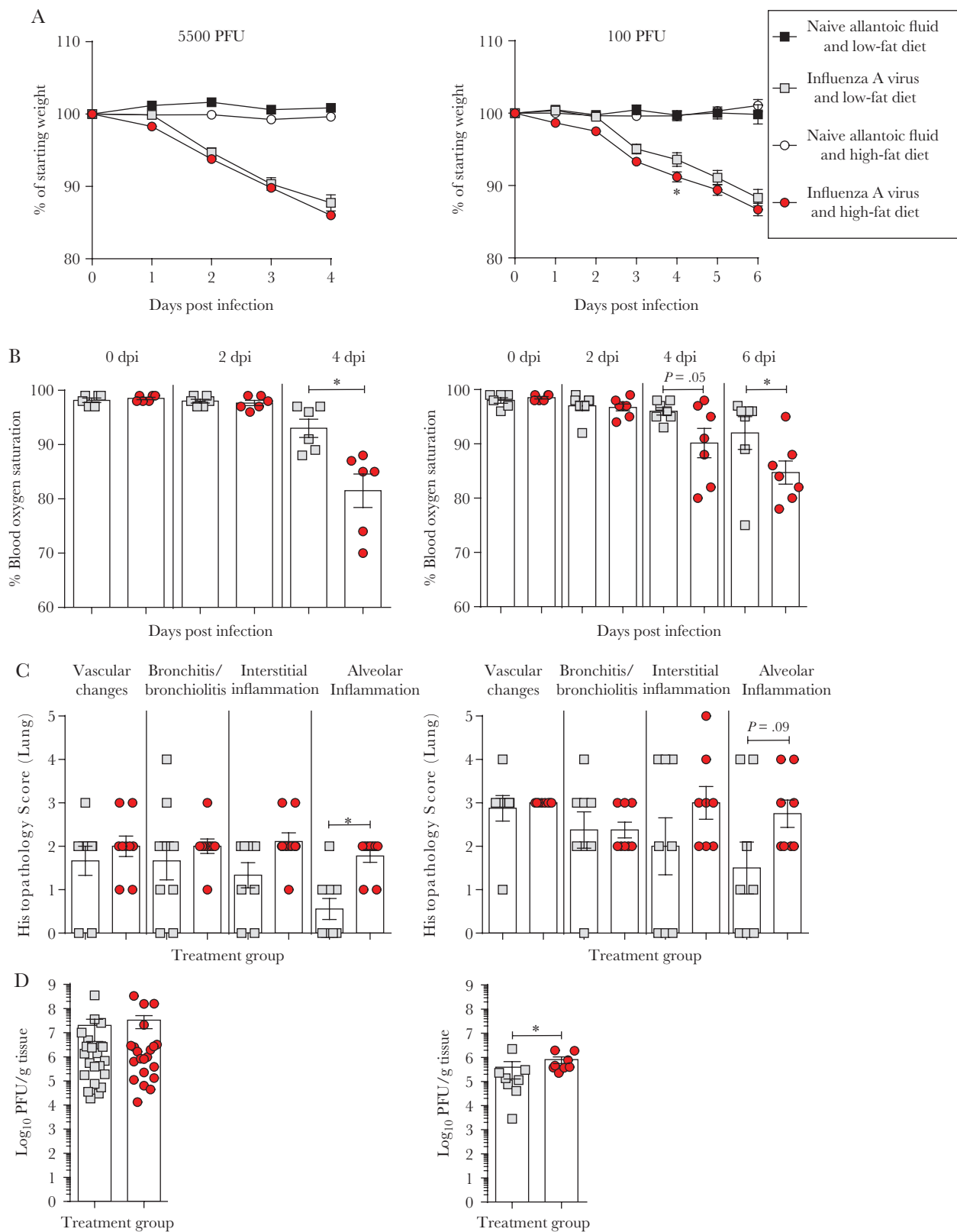


Figure 1. Mice fed a high-fat diet are more susceptible to severe respiratory disease following influenza A virus (Auckland/09) inoculation. (A) Weight loss, (B) percentage blood oxygen, (C) histopathological examination of pulmonary inflammation, and (D) pulmonary PFU of mice following inoculation with either 5500 PFU (left) or 100 PFU (right) of Auckland/09. Unless otherwise indicated, data were obtained at 4 dpi (5500 PFU) or 6 dpi (100 PFU). All graphs show the mean and standard error of mean of data pooled from at least 2 independent experiments. Statistical analysis was performed as described in "Materials and Methods" with $*P < .05$. Abbreviations: dpi, days post infection; PFU, plaque forming unit.

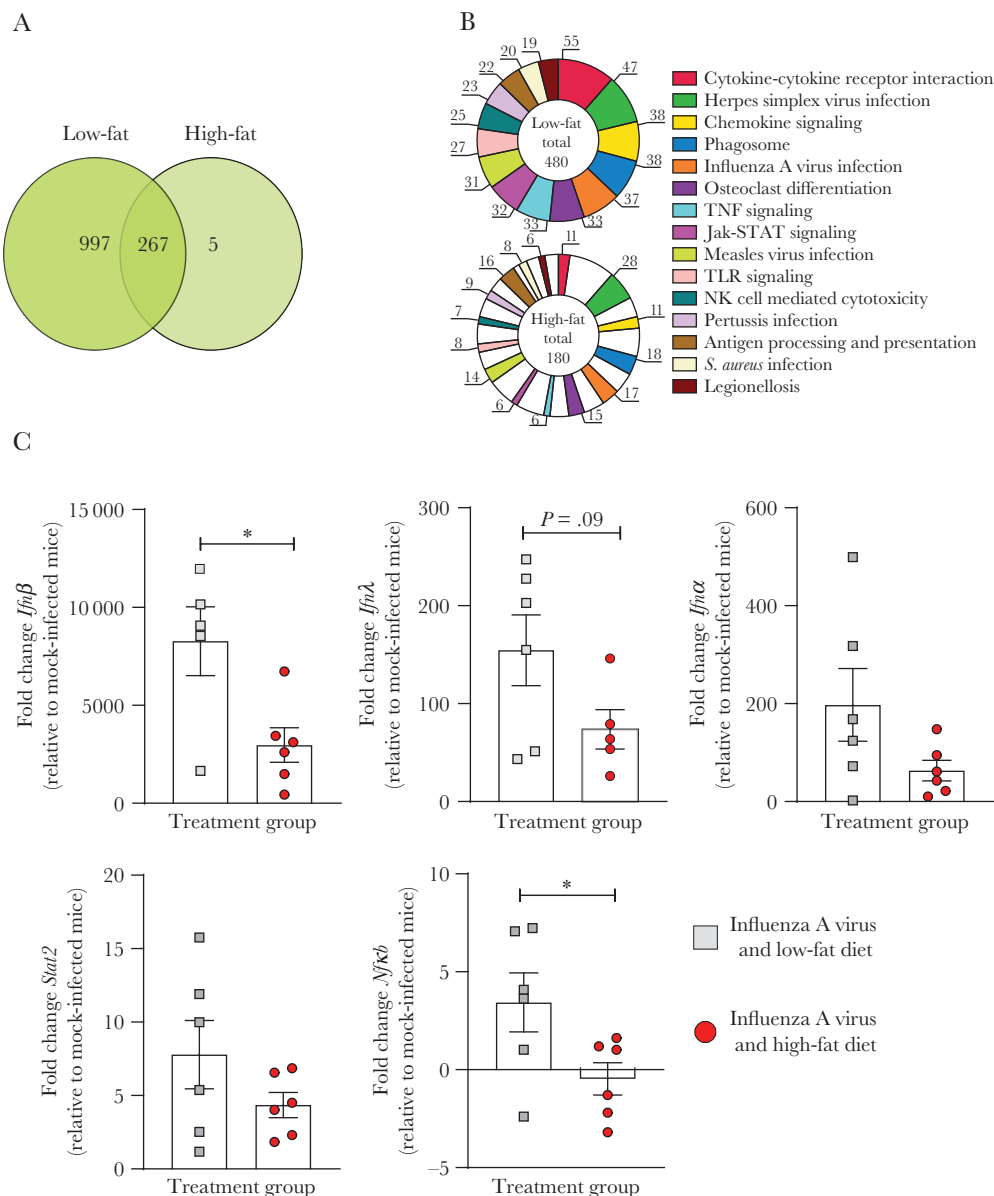


Figure 2. Reduced expression of inflammatory genes after IAV (Auckland/09) infection in the lungs of HF mice compared to the lungs of LF mice. *A*, Venn diagram of differentially expressed genes in IAV-infected LF and HF mice at 2 dpi (5500 PFU). *B*, The top 15 KEGG pathways identified in the analysis of the differentially expressed genes. *C*, qPCR analysis for different proinflammatory genes at 2 dpi (5500 PFU). All qPCR graphs show the mean and standard error of mean of data pooled from at least 2 independent experiments. Statistical analysis was performed as described in “Materials and Methods” with * $P < .05$. Abbreviations: dpi, days post infection; HF, high fat; IAV, influenza A virus; LF, low fat; NK cell, natural killer cell; PFU, plaque forming unit; qPCR, quantitative polymerase chain reaction; TLR, Toll-like receptor; TNF, tumor necrosis factor.

higher viral loads were detected in the hearts of HF mice compared to LF mice at 6 dpi (Figure 4A).

To differentiate locally replicating virus from infectious virions simply present in the organ of interest, qPCR for viral mRNA was performed (Figure 4B). Viral mRNA could be detected in the hearts of infected mice at 2 dpi (5500 PFU), although the amount of mRNA detected was not significantly different between LF and HF mice (Figure 4B). In contrast, at 6 dpi (100 PFU) there was significantly more viral mRNA in the hearts of IAV-infected HF mice compared to IAV-infected LF mice (Figure 4B).

To investigate the early host response to IAV in the heart, the transcriptome of the heart of IAV-infected LF and HF mice was assessed by RNASeq at 2 dpi (5500 PFU) (Supplementary Figure 3). Consistent with our previous analysis of the lung, there was a difference in gene expression between the hearts of uninfected LF and HF mice (Supplementary Table 3). However, as the focus of this study is the specific effects of IAV in HF and LF mice, all subsequent analyses were performed relative to the relevant uninfected controls. In the heart, genes differentially expressed in infected LF mice were also expressed to a lower level, or not at all, in infected HF mice (Figure 5A). Moreover, with the exception of *Entpd4*,

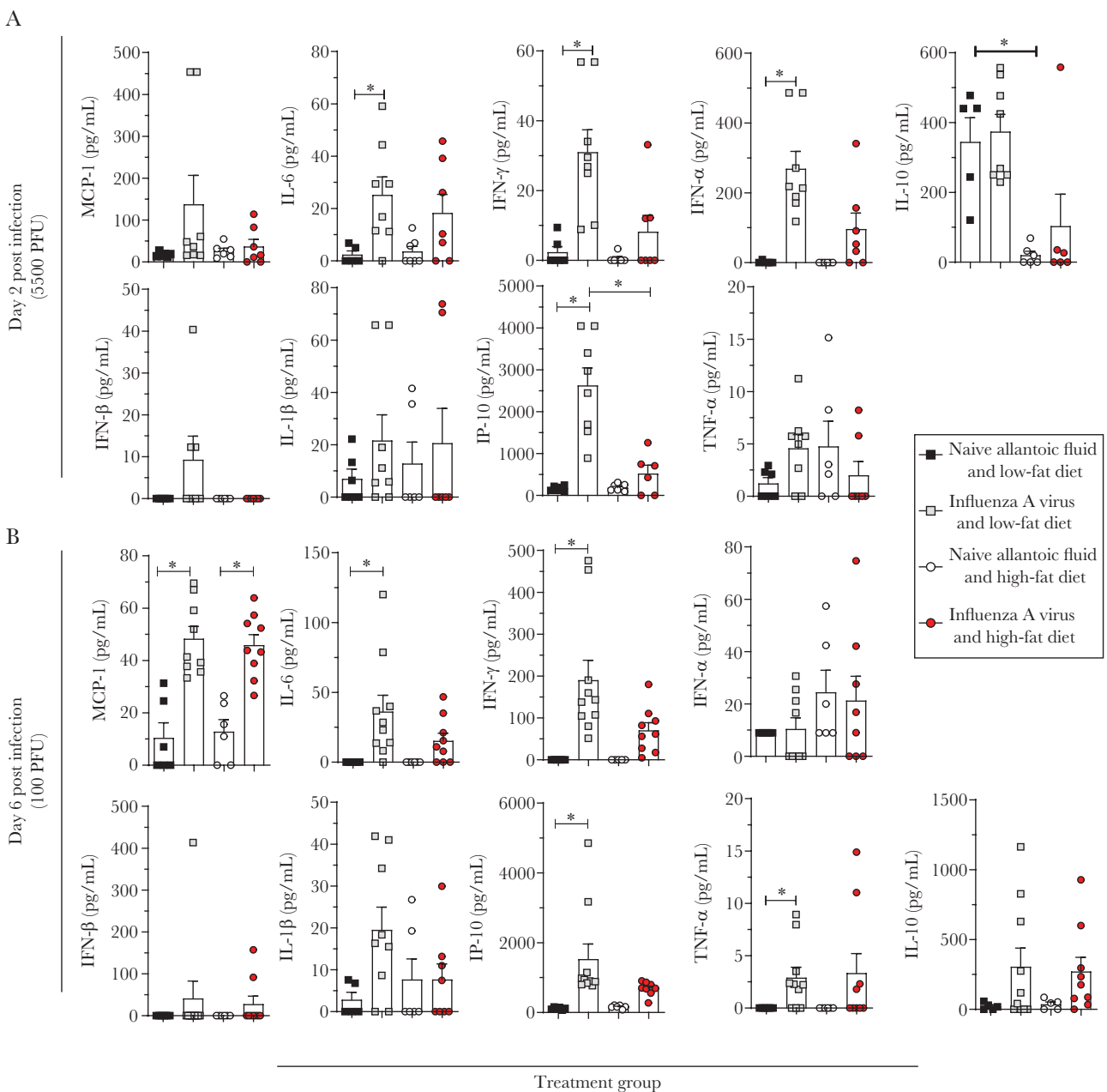


Figure 3. LF mice have a more pronounced proinflammatory response in the serum follow influenza A virus (Auckland/09) infection compared to HF mice. Data were obtained at (A) 2 dpi (following infection with 5500 PFU of virus) and (B) 6 dpi (following infection with 100 PFU of virus). All graphs show mean and standard error of mean of data pooled from at least 2 independent experiments. Statistical analysis was performed as described in the “Materials and Methods” with $*P < .05$. Abbreviations: dpi, days post infection; HF, high fat; IFN, interferon; IL, interleukin; IP-10, IFN- γ inducible protein-10; LF, low fat; MCP-1, monocyte chemoattractant protein-1; PFU, plaque forming unit; TNF, tumor necrosis factor.

differentially expressed genes in infected HF mice were also differentially expressed in infected LF mice (Figure 5A). Consistent with our previous observations in the lung (Figure 2), the majority of differentially expressed genes identified in infected LF mice belonged to pathways associated with the inflammatory response (Figure 5B). To determine if this gene expression profile (reduced proinflammatory and antiviral genes) was specific to this particular viral infectious dose/time point, the expression of key genes identified by RNASeq was assessed by qPCR at both 4 dpi (5500 PFU)

and 6 dpi (100 PFU) (Figure 5C). Consistent with the RNASeq data at 2 dpi, at 4 and 6 dpi IAV-infected LF mice had higher relative expression of *Irf7*, *Isg15*, and *Il-1 β* in the heart compared to IAV-infected HF mice (Figure 5C).

Changes in the Structural Status of the Heart of IAV-Infected HF Mice

The presence of viral mRNA in the hearts of infected mice, and the strong transcriptional response observed in the same organ, suggested that IAV may affect cardiac function. To determine if

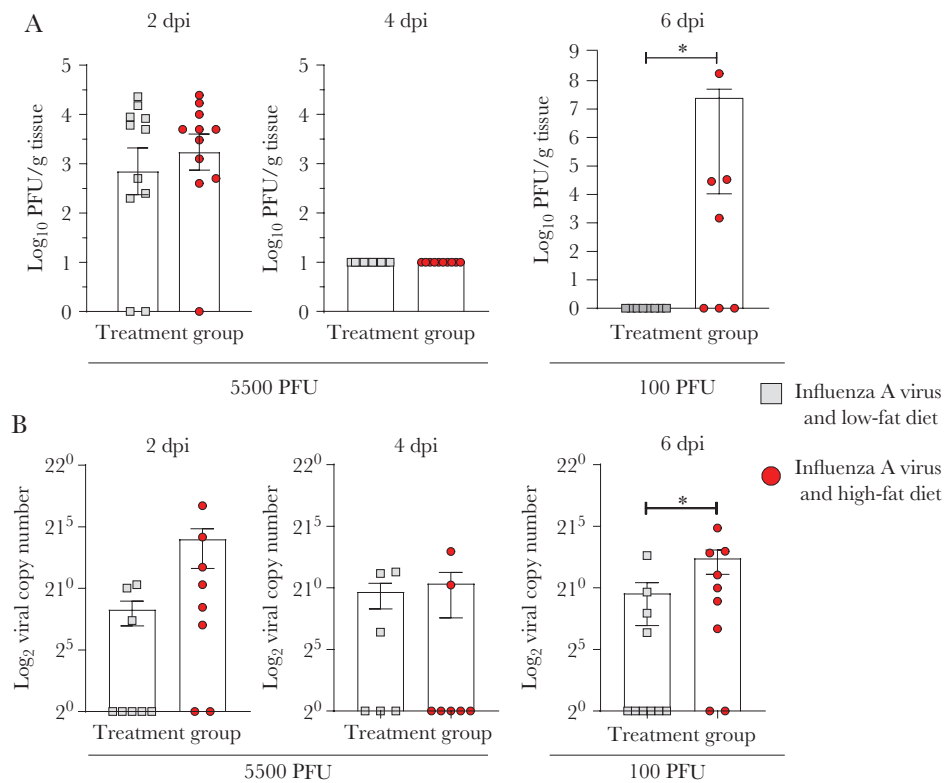


Figure 4. Influenza A virus (Auckland/09) can be detected in the hearts of LF and HF mice. *A*, Viral PFU in the heart of LF and HF mice at 2 dpi (following infection with 5500 PFU of virus) and 6 dpi (following infection with 100 PFU of virus). *B*, Viral mRNA in the heart of LF and HF mice at 2 dpi (following infection with 5500 PFU of virus) and 6 dpi (following infection with 100 PFU of virus). All graphs show mean and standard error of mean of data pooled from at least 2 independent experiments. Statistical analysis was performed as described in the “Materials and Methods” with * $P < .05$. Abbreviations: dpi, days post infection; HF, high fat; LF, low fat; PFU, plaque forming units.

this was the case, echocardiography was performed on LF and HF mice at 4 dpi (5500 PFU). There was no significant difference in various measures of cardiac function after IAV infection in both LF and HF mice when compared to their NAF-infected counterpart (Table 1). In contrast, IAV-infected HF mice had a significantly thicker left posterior ventricular wall compared to both IAV-infected LF mice and NAF-infected HF mice (Table 1). Similarly, IAV-infected HF mice had a significantly greater left ventricular mass compared to both IAV-infected LF mice and NAF-infected HF mice (Table 1). In contrast, in LF mice, IAV virus induced a significant *decrease* in left ventricular mass relative to NAF-infected LF mice (Table 1). To confirm these data, histology was used to assess left ventricle thickness at 4 dpi in IAV-infected LF and HF mice. Consistent with the echocardiographic data, IAV-infected HF mice had significantly thicker left ventricles than IAV-infected LF (Figure 6A), whilst a trend was seen towards increased left ventricle thickness in IAV-infected HF mice relative to NAF-infected HF mice. In contrast, there was no notable difference in the left ventricular mass of infected and uninfected LF mice (Figure 6A; $P > .99$).

To further investigate cardiomyopathy in these mice, heart sections were assessed for cardiomyocyte degeneration. Hearts from NAF-infected LF mice had no obvious histological abnormalities (Figure 6B). IAV-infected LF mice had signs of

mild cardiomyopathy, with some samples showing mild, focal cardiomyocyte degeneration (Figure 6B). In contrast to NAF-infected LF mice, hearts from NAF-infected HF mice typically showed minimal cardiomyocyte degeneration with scattered and small clusters of hyalinized cardiomyocytes detected in the majority of samples (Figure 6B). However, the HF IAV-infected mice were the only treatment group where widespread and extensive cardiomyocyte degeneration was observed (Figure 6B). None of these lesions had a focal association with active virus replication, based on the lack of AIV nucleoprotein detected at the exact same site of the lesion in a serial tissue section (data not shown).

Increased HIF-1 α in the Hearts of HF Mice After IAV Infection

HIF-1 α expression in the heart has been associated with cardiomyopathy and increased left ventricular mass, and implicated in the pathogenesis of cardiovascular disease [32, 33]. Given the structural changes observed in the hearts of HF mice after IAV infection, we sought to determine if this was associated with increased HIF-1 α expression in the heart. Accordingly, sections of murine hearts were immunolabeled for HIF-1 α at 4 dpi (following infection with 5500 PFU Auckland/09) and semiquantitatively assessed by a veterinary pathologist who was blinded to the respective treatment groups. Consistent with the observed structural changes, the hearts of HF

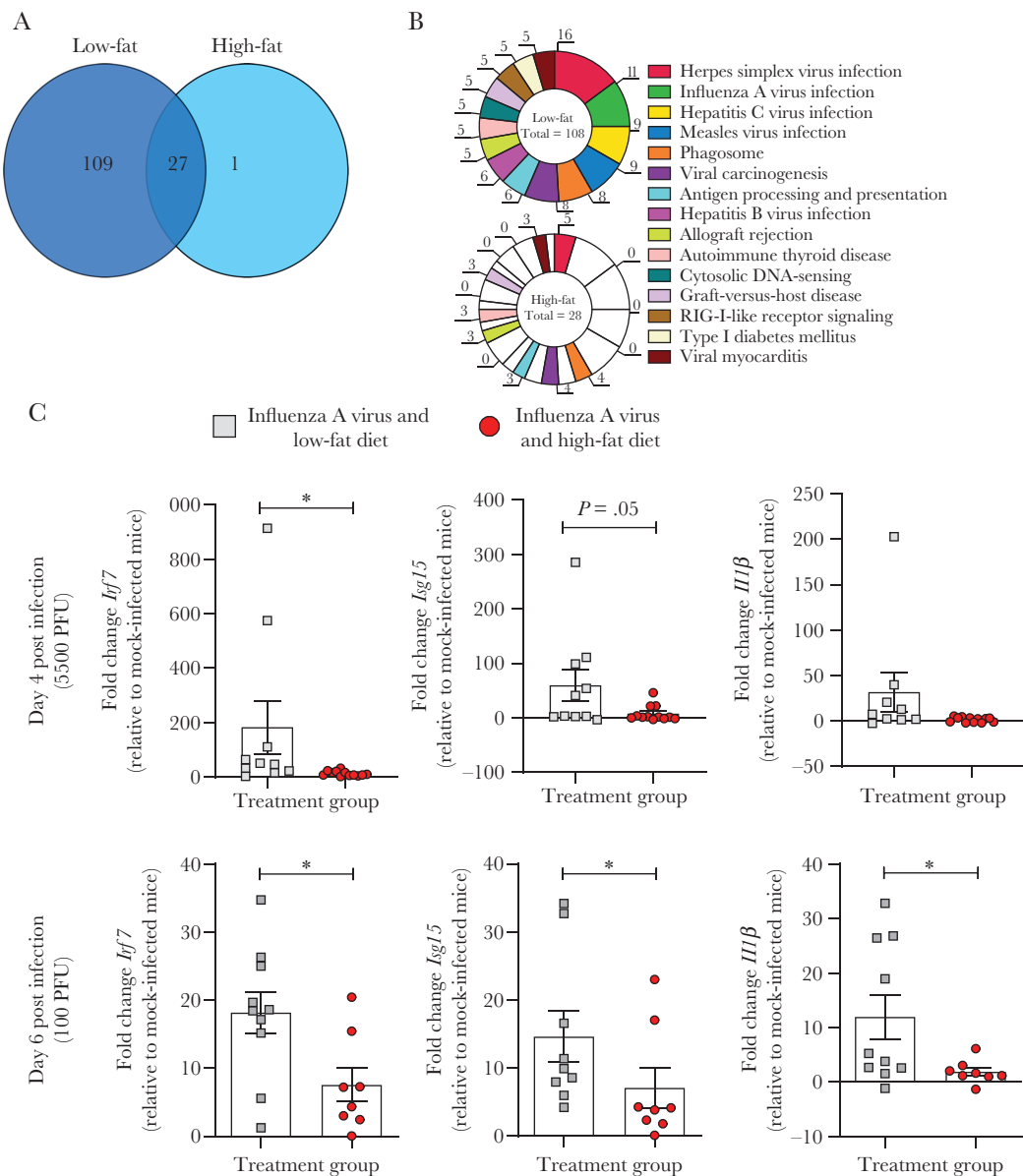


Figure 5. Reduced expression of inflammatory genes after influenza A virus (Auckland/09) infection in the hearts of HF mice compared to the hearts of LF mice. *A*, Venn diagram of differentially expressed genes in influenza A virus-infected LF and HF mice at 2 dpi (5500 PFU). *B*, KEGG pathway analysis of the differentially expressed genes. *C*, qPCR analysis for different proinflammatory genes at 4 dpi (5500 PFU) or 6 dpi (100 PFU). All qPCR graphs show the mean and standard error of mean of data pooled from at least 2 independent experiments. Statistical analysis was performed as described in the “Materials and Methods” with * $P < .05$. Abbreviations: dpi, days post infection; HF, high fat; LF, low fat; PFU, plaque forming units; qPCR, quantitative polymerase chain reaction.

infected mice had increased HIF-1 α immunolabelling compared to both their LF infected ($P < .05$) and naive HF counterparts ($P = .09$) (Figure 6C).

An Elevated BMI Is Associated With an Increased Risk of Influenza-Associated Cardiac Complications

Finally, we sought to validate the observations from our murine model of disease in the human population. To do so, we analyzed previously published data [22–25]. In all studies an increased percentage of overweight patients (compared to

patients with a healthy BMI) experienced a cardiovascular complication of IAV. This association was statistically significant in 2 of the 4 surveyed studies (Supplementary Table 4). Taken together, these data suggest that the role of excess weight in the cardiac complications of influenza in patients warrants further investigation.

DISCUSSION

Here, we showed that the systemic pathogenesis of influenza differs between HF mice and LF mice.

Table 1. Cardiovascular Parameters Measured by Echocardiogram at 4 dpi (Infectious Dose: 5500 PFU)

	Low Fat		High Fat	
	Mock (n = 8)	IAV (n = 10)	Mock (n = 8)	IAV (n = 9)
Global parameters				
Body weight, g	316±3.2	25.6±3.6	-19%	43.2±3 ^a
Heart rate, bpm	407.6±68.6	334.6±81.6	-18%	403.9±51.3
Functional status of the heart				
Cardiac output, mL/min	12.7±2.4	10.8±8.7	-15%	13.3±1.8
Ejection Fraction, %	47.4±8.6	55.8±11.7	+18%	57.5±4
Stroke Volume	31.3±4.9	26.8±8.6	-17%	33.1±2.9
Structural status of the heart				
LVAW-s, mm	1.2±0.2	1.2±0.2	0	1.2±0.1
LVPW-s, mm	1.2±0.2	1.2±0.2	0	1.1±0.1
LV mass, g	135.9±16.6	104.6±19.1 ^b	-23%	108.8±11
				135.7±29 ^{b,c}
				+25%

^a $P < .05$ vs mock treated, low fat mice (Kruskal-Wallis with Dunn's multiple comparison test).

^b $P < .05$ vs mock treated mice (same treatment group) (One-Way ANOVA with Sidak's multiple comparison test).

^c $P < .05$ vs IAV inoculated, low fat mice (One-Way ANOVA with Sidak's multiple comparison test).

Specifically, our data demonstrate that mice fed a high-fat diet had impairments in systemic inflammatory signaling in the lungs, circulation, and heart after IAV infection. This was associated with increased viral titers, cardiomyocyte degeneration, and increased Hif-1 α expression in the hearts of infected HF mice.

Impairments in the inflammatory response to IAV have previously been described in the lungs of HF mice [27]. Our data are the first to comprehensively characterize this pulmonary response early during infection (2 dpi) and demonstrate that these immune changes also occur outside of the respiratory tract. The exact trigger of the inflammatory transcriptome observed in the hearts of IAV-infected mice remains unclear. Given that we detected infectious virions in the hearts of both infected LF and HF mice, the associated inflammatory response could be a direct response to virus and/or viral antigens. This would be consistent with previous reports of viral antigen in the hearts of IAV-infected patients and mice [34–36]. Alternatively, the observed transcriptome could be induced indirectly, that is via exposure to proinflammatory mediators in blood that have been generated in response to the pulmonary infection. Regardless of the mechanism, the impaired cardiac inflammatory response in HF mice was associated with increased viral replication in the hearts of these mice at later time points post infection. This is consistent with recent findings that in the absence of IFITM3, there is increased IAV replication in the hearts of mice [37].

The altered transcriptome and increased viral replication in the hearts of HF mice was further associated with increased left ventricular mass and thickening of the left ventricle posterior wall. At present, the precise mechanism(s) by which influenza increases left ventricular mass in HF mice remains to be defined. Increased left ventricular mass can be the result of numerous different physiological changes, including increased cardiomyocyte mass, endothelial cell proliferation, fibrosis, and/or inflammatory signaling/immune cell activation [38]. Several studies have shown that IFN- γ plays a protective role in the development of cardiac hypertrophy [39–42]. Because HF mice fail to induce similar levels of IFN- γ relative to LF mice, it is possible that this drove the observed increase in left ventricular mass. Alternatively, it is possible that as IAV causes hypoxemia in HF mice, this triggered cardiac hypoxia and increased left ventricular mass [43–45]. It is also important to note that whilst left ventricular function is a critical parameter in predicting cardiac morbidity and mortality [38], RV function is a more clinically relevant and sensitive measurement to examine the pathological changes associated with the cardiopulmonary diseases (ie, influenza). Unfortunately, consistent and reproducible echocardiographic evaluation of the RV is inherently difficult due to its retrosternal position and crescent-shaped structure [46]. It is therefore important for future studies to overcome these technical limitations and investigate RV function in both HF and LF mice.

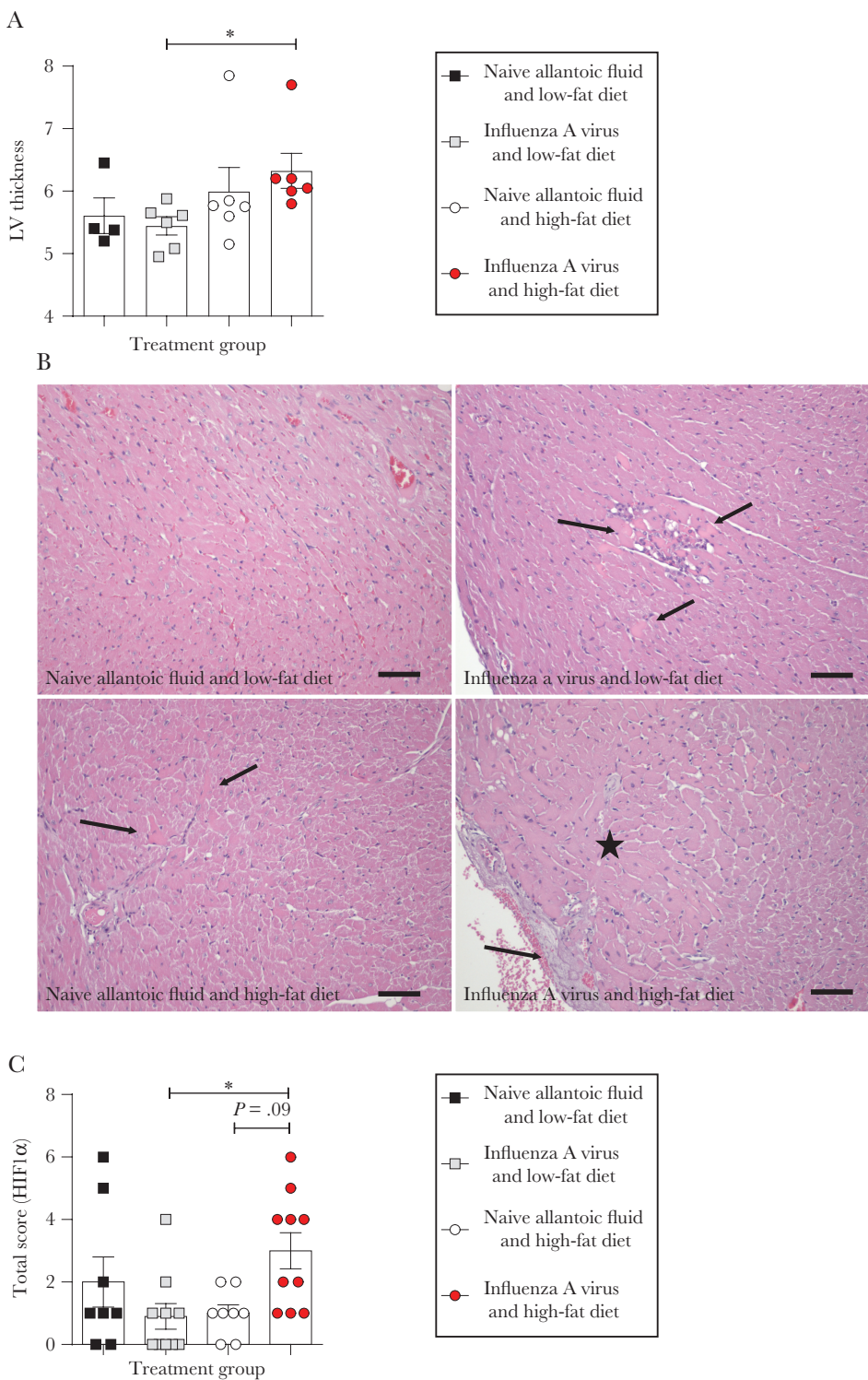


Figure 6. Structural changes in the hearts of IAV-infected HF mice. *A*, Left ventricle thickness (arbitrary units) at 4 dpi following infection with 5500 PFU of Auckland/09(H1N1). Graph shows the mean and standard error of mean and data are representative of 2 independent experiments. *B*, Representative images of cardiomyocyte degeneration in the hearts of IAV- and NAF-infected LF and HF mice. Top left: Histologically normal heart from NAF-infected LF mouse. Top right: heart from IAV-infected LF mouse. There are scattered and small clusters of degenerating cardiomyocytes (arrows). Bottom left: Heart from NAF-infected HF mouse showing randomly scattered but relatively rare degenerating cardiomyocytes. Bottom right: Heart from IAV-infected HF mice. There is focally severe cardiomyocyte degeneration (star), mild perivascular edema, and a small fibrin-thrombus attached to the endocardium of the left ventricle (arrow). Images are representative of $n > 5$ per group (100 μ m). *C*, Increased HIF-1 α in the hearts of IAV-infected HF mice. Graph shows the mean and standard error of mean of data pooled from a minimum of 2 independent experiments. Statistical analysis in (*A*) and (*C*) was performed as described in the “Materials and Methods” with $*P < .05$. Abbreviations: dpi, days post infection; HF, high fat; IAV, influenza A virus; LF, low fat; LV, left ventricle; NAF, naive allantoic fluid.

Mice can never fully recapitulate the complexity of disease that occurs in the human population. We therefore sought to validate the observed association between excess weight and the cardiovascular complications of IAV across a variety of different published clinical studies. Unfortunately, of those studies that were available and recorded the cardiovascular complications of influenza, few also recorded patient BMI, therefore reducing the power of the analysis. Similarly, in the absence of a specifically designed clinical study, it is not possible to assess the rate of spontaneous cardiovascular disease in overweight patients (ie, in the absence of IAV). Nevertheless, in all 4 clinical studies that were obtained and had recorded the relevant data, a higher percentage of cardiovascular complications were recorded in influenza patients who had excess weight compared to those with a healthy BMI. This association was statistically significant in 2 of the 4 available studies. Whilst these data are certainly not definitive, they do suggest that there is sufficient preliminary evidence to warrant a targeted clinical assessment of the role of excess weight in the extrarespiratory complications of influenza and other infectious diseases. When one considers the fact that it is now predicted that in the year 2030 nearly 1 in 2 US adults will be living with obesity [47], a complete understanding of the role of excess weight in the cardiac complications of IAV becomes particularly pertinent.

Supplementary Data

Supplementary materials are available at *The Journal of Infectious Diseases* online. Consisting of data provided by the authors to benefit the reader, the posted materials are not copyedited and are the sole responsibility of the authors, so questions or comments should be addressed to the corresponding author.

Notes

Financial support. This work was supported by the Erasmus Trust Fund Foundation (grant to J. Y. S.); the Netherlands Organization for Scientific Research (grant numbers 91614115 and 91718308 to D. v. R.); the Erasmus Medical Center Foundation (grant to D. v. R.); and the Australian Research Council (grant number DE180100512 to K. R. S.). The Preclinical Imaging Facility, Translational Research Institute is supported by the Australian Research Council (grant number LE150100067) and the Australian Federal Government.

Potential conflicts of interest. All authors: No reported conflicts of interest. All authors have submitted the ICMJE Form for Disclosure of Potential Conflicts of Interest. Conflicts that the editors consider relevant to the content of the manuscript have been disclosed.

References

- Van Kerkhove MD, Hirve S, Koukounari A, Mounts AW; H1N1pdm Serology Working Group. Estimating age-specific cumulative incidence for the 2009 influenza pandemic: a meta-analysis of A (H1 N 1) pdm09 serological studies from 19 countries. *Influenza Other Respir Viruses* 2013; 7:872–6.
- Díaz E, Rodríguez A, Martín-Loeches I, et al. Impact of obesity in patients infected with 2009 influenza A (H1N1). *Chest* 2011; 139:382–6.
- Gill JR, Sheng ZM, Ely SF, et al. Pulmonary pathologic findings of fatal 2009 pandemic influenza A/H1N1 viral infections. *Arch Pathol Lab Med* 2010; 134:235–43.
- Louie JK, Acosta M, Samuel MC, et al; California Pandemic (H1N1) Working Group. A novel risk factor for a novel virus: obesity and 2009 pandemic influenza A (H1N1). *Clin Infect Dis* 2011; 52:301–12.
- Morgan OW, Bramley A, Fowlkes A, et al. Morbid obesity as a risk factor for hospitalization and death due to 2009 pandemic influenza A(H1N1) disease. *PLoS One* 2010; 5:e9694.
- Louie JK, Acosta M, Winter K, et al; California Pandemic (H1N1) Working Group. Factors associated with death or hospitalization due to pandemic 2009 influenza A(H1N1) infection in California. *JAMA* 2009; 302:1896–902.
- Rothberg MB, Haessler SD. Complications of seasonal and pandemic influenza. *Crit Care Med* 2010; 38:e917.
- Bautista E, Chotpitayasunondh T, Gao Z, et al; Writing Committee of the WHO Consultation on Clinical Aspects of Pandemic (H1N1) 2009 Influenza. Clinical aspects of pandemic 2009 influenza A (H1N1) virus infection. *N Engl J Med* 2010; 362:1708–19.
- Smith AG, Sheridan PA, Harp JB, Beck MA. Diet-induced obese mice have increased mortality and altered immune responses when infected with influenza virus. *J Nutr* 2007; 137:1236–43.
- Karlsson EA, Beck MA. The burden of obesity on infectious disease. *Exp Biol Med (Maywood)* 2010; 235:1412–24.
- Teran-Cabanillas E, Montalvo-Corral M, Caire-Juvera G, Moya-Camarena SY, Hernández J. Decreased interferon- α and interferon- β production in obesity and expression of suppressor of cytokine signaling. *Nutrition* 2013; 29:207–12.
- Sellers SA, Hagan RS, Hayden FG, Fischer WA 2nd. The hidden burden of influenza: a review of the extra-pulmonary complications of influenza infection. *Influenza Other Respir Viruses* 2017; 11:372–93.
- Siriwardena AN. Increasing evidence that influenza is a trigger for cardiovascular disease. *J Infect Dis* 2012; 206:1636–8.
- Smeeth L, Thomas SL, Hall AJ, Hubbard R, Farrington P, Vallance P. Risk of myocardial infarction and stroke after acute infection or vaccination. *N Engl J Med* 2004; 351:2611–8.
- Warren-Gash C, Hayward AC, Hemingway H, et al. Influenza infection and risk of acute myocardial infarction in England and Wales: a CALIBER self-controlled case series study. *J Infect Dis* 2012; 206:1652–9.
- Kwong JC, Schwartz KL, Campitelli MA, et al. Acute myocardial infarction after laboratory-confirmed influenza infection. *N Engl J Med* 2018; 378:345–53.

17. Chooi YC, Ding C, Magkos F. The epidemiology of obesity. *Metabolism* **2019**; 92:6–10.
18. Short KR, Diavatopoulos DA, Reading PC, et al. Using bioluminescent imaging to investigate synergism between *Streptococcus pneumoniae* and influenza A virus in infant mice. *J Vis Exp* **2011**; (50):e2357.
19. Bielefeldt-Ohmann H, Tolnay AE, Reisenhauer CE, Hansen TR, Smirnova N, Van Campen H. Transplacental infection with non-cytopathic bovine viral diarrhoea virus types 1b and 2: viral spread and molecular neuropathology. *J Comp Pathol* **2008**; 138:72–85.
20. Tolnay AE, Baskin CR, Tumpey TM, et al. Extrapulmonary tissue responses in cynomolgus macaques (*Macaca fascicularis*) infected with highly pathogenic avian influenza A (H5N1) virus. *Arch Virol* **2010**; 155:905–14.
21. Short KR, Reading PC, Brown LE, et al. Influenza-induced inflammation drives pneumococcal otitis media. *Infect Immun* **2013**; 81:645–52.
22. Beumer MC, Koch RM, van Beuningen D, et al. Influenza virus and factors that are associated with ICU admission, pulmonary co-infections and ICU mortality. *J Crit Care* **2019**; 50:59–65.
23. Pawelka E, Karolyi M, Daller S, et al. Influenza virus infection: an approach to identify predictors for in-hospital and 90-day mortality from patients in Vienna during the season 2017/18. *Infection* **2020**; 48:51–6.
24. Pizzini A, Burkert F, Theurl I, Weiss G, Bellmann-Weiler R. Prognostic impact of high sensitive troponin T in patients with influenza virus infection: a retrospective analysis. *Heart Lung* **2020**; 49:105–9.
25. Dunning J, Blankley S, Hoang LT, et al; MOSAIC Investigators. Progression of whole-blood transcriptional signatures from interferon-induced to neutrophil-associated patterns in severe influenza. *Nat Immunol* **2018**; 19:625–35.
26. Zheng W, McLellan DF, Rolland B, et al. Association between body-mass index and risk of death in more than 1 million Asians. *N Engl J Med* **2011**; 364:719–29.
27. Honce R, Schultz-Cherry S. Impact of obesity on influenza A virus pathogenesis, immune response, and evolution. *Front Immunol* **2019**; 10:1071.
28. Nieman DC, Henson DA, Nehlsen-Cannarella SL, et al. Influence of obesity on immune function. *J Am Diet Assoc* **1999**; 99:294–9.
29. Mancuso P. Obesity and respiratory infections: does excess adiposity weigh down host defense? *Pulm Pharmacol Ther* **2013**; 26:412–9.
30. Andersen CJ, Murphy KE, Fernandez ML. Impact of obesity and metabolic syndrome on immunity. *Adv Nutr* **2016**; 7:66–75.
31. O'Brien KB, Vogel P, Duan S, et al. Impaired wound healing predisposes obese mice to severe influenza virus infection. *J Infect Dis* **2012**; 205:252–61.
32. Gao T, Zhu ZY, Zhou X, Xie ML. *Chrysanthemum morifolium* extract improves hypertension-induced cardiac hypertrophy in rats by reduction of blood pressure and inhibition of myocardial hypoxia inducible factor-1alpha expression. *Pharm Biol* **2016**; 54:2895–900.
33. Czibik G. Complex role of the HIF system in cardiovascular biology. *J Mol Med (Berl)* **2010**; 88:1101–11.
34. Pan HY, Yamada H, Chida J, et al. Up-regulation of ectopic trypsin in the myocardium by influenza A virus infection triggers acute myocarditis. *Cardiovasc Res* **2011**; 89:595–603.
35. Ray CG, Icenogle TB, Minnich LL, Copeland JG, Grogan TM. The use of intravenous ribavirin to treat influenza virus-associated acute myocarditis. *J Infect Dis* **1989**; 159:829–36.
36. Davoudi AR, Maleki AR, Beykmohammadi AR, Tayebi A. Fulminant myopericarditis in an immunocompetent adult due to pandemic 2009 (H1N1) influenza A virus infection. *Scand J Infect Dis* **2012**; 44:470–2.
37. Kenney A, McMichael TM, Imas A, et al. IFITM3 protects the heart during influenza virus infection. *Proc Natl Acad Sci U S A* **2019**; 116:18607–12.
38. Frieler RA, Mortensen RM. Immune cell and other noncardiomyocyte regulation of cardiac hypertrophy and remodeling. *Circulation* **2015**; 131:1019–30.
39. Kimura A, Ishida Y, Furuta M, et al. Protective roles of interferon- γ in cardiac hypertrophy induced by sustained pressure overload. *J Am Heart Ass* **2018**; 7:e008145.
40. Garcia AG, Wilson RM, Heo J, et al. Interferon- γ ablation exacerbates myocardial hypertrophy in diastolic heart failure. *Am J Physiol Heart Circ Physiol* **2012**; 303:H587–96.
41. Jin H, Li W, Yang R, Ogasawara A, Lu H, Paoni NF. Inhibitory effects of interferon-gamma on myocardial hypertrophy. *Cytokine* **2005**; 31:405–14.
42. Liu YY, Cai WF, Yang HZ, et al. Bacillus Calmette-Guérin and TLR4 agonist prevent cardiovascular hypertrophy and fibrosis by regulating immune microenvironment. *J Immunol* **2008**; 180:7349–57.
43. Takimoto E, Kass DA. Role of oxidative stress in cardiac hypertrophy and remodeling. *Hypertension* **2007**; 49:241–8.
44. Avelar E, Cloward TV, Walker JM, et al. Left ventricular hypertrophy in severe obesity: interactions among blood pressure, nocturnal hypoxemia, and body mass. *Hypertension* **2007**; 49:34–9.
45. Yamashita C, Hayashi T, Mori T, et al. Angiotensin II receptor blocker reduces oxidative stress and attenuates hypoxia-induced left ventricular remodeling in apolipoprotein E-knockout mice. *Hypertension Res* **2007**; 30:1219–30.
46. Markley RR, Ali A, Potfay J, Paulsen W, Jovin IS. Echocardiographic evaluation of the right heart. *J Cardiovasc Ultrasound* **2016**; 24:183–90.
47. Ward ZJ, Bleich SN, Cradock AL, et al. Projected US state-level prevalence of adult obesity and severe obesity. *N Engl J Med* **2019**; 381:2440–50.